

Processing and Characterization of Proton Conducting Material Based on Cerate-Zirconate Ceramics

Nafisah Osman^{a,b,*}, Nur Syafkeena Mohd Affandi^b, Oskar Hasdinor Hassan^c

^aPhysics Department, Faculty of Applied Sciences, Universiti Teknologi MARA, 02600 Arau, Perlis, Malaysia

^bProton Conducting Fuel Cell Research Group, Faculty of Applied Sciences,

^cFaculty of Art & Design,

Universiti Teknologi MARA, 40450 Shah Alam, Selangor, Malaysia

*Corresponding author: fisha@uitm.edu.my

Received 19 July 2019, Received in revised form 15 November 2019

Accepted 30 December 2019, Available online 28 February 2020

ABSTRACT

Solid electrolyte based on cerate-zirconates have been widely investigated world-wide as proton conductor for potential applications in electrochemical devices such as fuel cells, electrochemical sensors, reactors, and devices. The most conventional physical method to prepare these ceramic electrolytes is via solid-state reaction (SSR). However, chemical method or known as wet chemical method (WCM) such as a sol-gel process has become a reliable route in terms of producing high purity and homogenous ultrafine powders. Tailoring the microstructure of the ceramics electrolyte can be achieved as sol gel process produces single perovskite phase of cerate-zirconates at lower processing temperature. This lower heat treatment produces the ceramics with improved quality for instance ultra-fine and agglomerate free powders with narrow size distributions. Subsequently, the innovative procedures generates high relative density of the electrolyte with improved quality and performance. Within the scope, in this paper we summarize our recent results on the synthesis of doped Ba(Ce,Zr)O₃ nanopowders by a modified sol-gel routes using metal nitrate salts as precursor.

Keywords: Modified sol-gel; nano particle; cerate-zirconate; chemical agent

ABSTRAK

Elektrolit pepejal berdasarkan serat-zirkonat telah banyak disiasat di seluruh dunia sebagai konduktor proton untuk aplikasi yang berpotensi dalam peranti elektrokimia seperti sel bahan bakar, sensor elektrokimia, reaktor, dan peranti. Kaedah fizikal konvensional untuk menyediakan elektrolit seramik ini adalah melalui tindak balas pepejal (SSR). Walau bagaimanapun, kaedah kimia atau dikenali sebagai kaedah kimia basah (WCM) seperti proses sol-gel telah menjadi kaedah yang boleh dipercayai untuk menghasilkan serbuk nano yang mempunyai ketulenan tinggi dan homogen. Mikrostruktur elektrolit seramik boleh diubah melalui proses sol-gel yang dapat menghasilkan fasa perovskite tunggal cerate-zirconates pada suhu pemprosesan yang lebih rendah. Ini kerana rawatan haba yang lebih rendah menghasilkan seramik dengan kualiti yang lebih baik contohnya serbuk ultra-halus dan bebas agglomerat dengan pengedaran saiz yang kecil. Selanjutnya, kaedah tersebut dapat menghasilkan elektrolit dengan kepadatan relatif tinggi berserta peningkatan kualiti dan prestasi. Di dalam kajian ini, kami merumuskan hasil kajian sintesis doped Ba(Ce, Zr)O₃ serbuk nano menggunakan kaedah sol-gel yang diubahsuai menggunakan garam nitrat logam sebagai pendahulu.

Kata kunci: Sol-gel ubah suai; zarah nano; serat-zirkonat; agen kimia

INTRODUCTION

A proton conductor is an electrolyte, typically a solid electrolyte, in which H⁺ are the primary charge carriers (Kreuer 2003). Proton conductors are most often made of polymers or ceramic. There has been a great deal of scientific and technological interest in developing improved systems using proton conductor such as portable electronic devices, backup power systems to electric vehicles, gas sensors, electro-chromic displays, and fuel cells (Baharuddin et al. 2018; Dziurdzia et al. 2015; Stambouli and Traversa

2002). In fuel cell system, a proton conductor usually found as an electrolyte materials in solid oxide fuel cell (SOFC) due to its remarkable performance at intermediate temperature (IT), so called as IT-SOFC. IT-SOFC offers wide range of materials selection to be operated at < 800 °C temperatures. In this type of SOFC or known as proton conducting fuel cell (PCFC), the electrolyte layer is usually a proton conducting oxide with ABO₃ perovskite structure. Proton-conducting electrolyte possess higher electrical conductivity in temperature ranging between 500 – 800 °C than conventional oxide-ion conducting electrolyte materials

(> 800 °C) (Kreuer 2003; Kreuer 1997). Moreover, due to the low activation energy required for proton conduction, proton conducting electrolyte is suitable to be used in this intermediate temperature regime (Kreuer 1999).

The established proton conductor based on perovskite structure, ABO_3 comprises of; A-site that can be fitted with Ca^{2+} , Sr^{2+} , Ba^{2+} ; and B-site with Ce^{4+} , Zr^{4+} . Each material possesses different conducting properties based on the combination of A-site with B-site cations. Among proven perovskite oxide materials, doped- $BaCeO_3$, and $BaZrO_3$ are the two most profoundly studied due to the excellence in protonic conductivity and chemical stability, respectively (Norman et al. 2018 & Baral et al. 2014). At present, research on doped barium cerate-zirconate perovskite oxide for example doped $Ba(Ce,Zr)O_3$ has gained the most attention in PCFC research. The improved version of barium-cerates and barium-zirconates with trivalent rare-earth element such as (Y^{3+}) doping has proved outstanding performance (Fu et al. 2010). The work done by Lyagaeva et al. (2016) also reported that the $BaCe_{0.5}Zr_{0.3}Y_{0.2}O_{3-\delta}$ shows higher protonic conductivity and lower contribution of p-type electronic conductivity.

Generally, the solid electrolyte is synthesized using the most conventional physical method, a solid-state reaction (SSR) (Ricote et al. 2012). Despite being simple, SSR retain a few challenges in terms of large particle size and low surface area powders (Biasotto et al. 2011). An alternative to conventional SSR method is the wet chemicals method. The term refers to a group of methods (including sol-gel and Pechini method) using liquid phase at one of the process stages. Sol-gel process is one of the simplest technique with advantages such as the ability to produce crystalline materials and nano particle powder at lower processing temperature besides shorter duration of phase formation (Liu et al. 2011).

Nowadays, further modification of the sol-gel process has been established by incorporating chemical agents such as chelating agent, surfactant, dispersing agent and polymerization agent. By adding such agents, the important parameters involve during synthesizing process for example pH, precursor type, catalyst and temperature can be controlled to tailor the microstructure of cerate-zirconates electrolyte with better electrical and mechanical properties. With these reasons, in this study, for the first approach we incorporated the addition of chelating agents into the sol-gel process. Mechanism process behind chelating agents are interaction of two or more binding sites between the chelates and a single central atom by forming a bond (Abdullah et al. 2012). This beneficial process prevents the formation of $BaCO_3$ that is usually yield during the synthesizing of cerate-based ceramics due to incomplete combustion as a result of the adsorption of CO_2 on the powder surface and transformed into CO_3 (Senari et al. 2017). The second approach is to make use of different surfactants during the synthesizing of cerate-zirconate ceramics in controlling the particle size, reducing the agglomeration of the particle as well as decreasing the processing temperature of the ceramic

(Mazlan et al. 2015). A work by Ke et al. (2015) revealed $Nd_2Si_2O_7$ powder had less aggregates and better dispersion than that of without surfactant during synthesizing process. Therefore, the aim of this study is to discuss on the processing and characterization of $BaCe_{0.54}Zr_{0.36}Y_{0.1}O_{3-\delta}$ proton conductor prepared by a modified sol-gel method using chelating agents and surfactants, respectively.

METHODOLOGY

Cerate-zirconate powders of $BaCe_{0.54}Zr_{0.36}Y_{0.1}O_{3-\delta}$ (BCZY) are prepared via a modified sol-gel method. The first route is by addition of various chelating agents (RA), and the second route involves in addition of various surfactants (RB). Metal nitrate precursors as listed ($Ba(NO_3)_2$ (99%, ACROS), $Ce(NO_3)_3$ (99.5%, ACROS), $Zr(NO_3)_2 \cdot O \cdot xH_2O$ (99.5%, ACROS) and $Y(NO_3)_3 \cdot 5H_2O$ (99.9%, ACROS) are used to prepare the BCZY powders.

RA. A stoichiometric amount of precursors materials are dissolved in deionized water on a hotplate, followed by the addition of citric acid. The mixture is stirred continuously and the chelating agents, triethylenetetraamine, TETA (RA1), and ethylenediaminetetraacetic acid, EDTA (RA2) are added. Next, a polymerizing agent (ethylene glycol) is added to the solution mixture. The ceramic powder was synthesized by the following ratio of metal nitrate to polymerization agent to chelating agent; 6:4:6. The process is completed by heating the solution mixture at temperature of 120-250 °C to form viscous gel. The gel is dried at 325 °C to produce black ash-sponge product and consequently calcined at 1100 °C for 10 h to yield a single phase BCZY powders. A detailed preparation on this route has been reported elsewhere (Mazlan et al. 2015).

RB. A stoichiometric amount of precursors materials are dissolved in deionized water on a hotplate. The mixture is stirred continuously followed by the addition of citric acid. Next, four types of surfactant are added individually; Brij-97 (RB1), Triton X-100 (RB2), Dimethyldioctadecylammonium chloride, DiDAC (RB3). Following that, ethylene glycol is added into the mixture. The ceramic powder was synthesized by the following ratio of surfactant to metal nitrate to polymerization agent to chelating agent; 1:6:4:6. The process is completed by heating the solution mixture at temperature of 120-250 °C to form viscous gel. The gel is dried at 325 °C to produce black ash-sponge product and consequently calcined at temperature between 900-1100 °C for 10 h to yield a single phase BCZY powders (Mazlan et al. 2015).

The phase identification of samples for RA and RB are completed using an X-ray diffractometer (Shimadzu XRD-6000) equipped with Ni-filtered and graphite monochromatized $Cu-K\alpha$ ($\lambda = 1.5406 \text{ \AA}$) over 2θ range from 20° to 70° with a step size of 0.02° s⁻¹. The samples for both routes are observed under field emission scanning electron microscope (FESEM) to evaluate the particles shapes and sizes. The single phase powders with smallest

particle and low agglomeration is pelletized and subjected to electrochemical impedance spectroscopy (EIS) analysis. Prior to the measurement, both surface of the pellet is polished and painted with platinum ink. Impedance measurement of the pellet is examined using EIS technique in wet nitrogen atmosphere via ZIVE SP2 Electrochemical workstation (ZIVELAB WonATech). The EIS measurement is taken over 100 mHz - 1 MHz frequency range at intermediate operating temperature limits with a 100 mV applied voltage. The data analyses are completed using Z-MAN Software to extract the possible electrical responses and the resistances are determined through the values obtained from the fitting procedure. Lastly, the cross-sectional view of the pellet after EIS measurement is observed using Benchtop SEM (Phenom XL).

RESULTS AND DISCUSSION

Figure 1 showed the XRD spectrum of RA1 and RA2 after calcined at $T=1100\text{ }^{\circ}\text{C}$. The selection of these two types of chelating agent is based on our previous works that amongst all chelating agents used in RA route are TETA (RA1) and EDTA (RA2). RA1 showed higher intensity and narrower peaks than that of RA2, which correspond to the high crystallinity of cubic structure of $\text{Ba}(\text{Ce,Zr})\text{O}_3$ (JCPDS 892485). The usage of TETA as chelating agents effectively hindered the formation of BaCO_3 in the final powders which lead to 100 wt% purity phase as compared to RA2 (94.42% purity phase). This is evidence from the XRD analysis that no impurity peaks are detected for RA1. TETA is an organic compounds grouped as amines, which contain a basic nitrogen atom with a lone pair. It exhibits strong coordinating ability towards metal ions due to the electron-donating activity of amine groups with a lone pair of electrons in nitrogen (Abdullah et al. 2018). Hence, TETA enable to bind with Ba^{2+} adequately (Reverchon et al. 2006). The absence of impurity in RA1 after calcined at $T=1100\text{ }^{\circ}\text{C}$ is also supported by the FTIR result as presented in insert

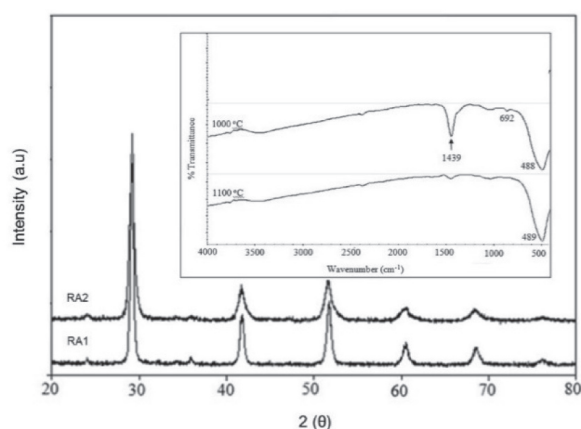


FIGURE 1. XRD patterns of BCZY powder of RA1 and RA2 after calcined at $T = 1100\text{ }^{\circ}\text{C}$. (Insert is FTIR results for RA1 after calcined at 1000 and 1100 $^{\circ}\text{C}$).

Figure 1. Further reduction of calcination temperature of RA to $T=1000\text{ }^{\circ}\text{C}$, the secondary phase of carbonate species is detected at 1439 cm^{-1} . Thus it manifested that the optimum temperature to produce pure phase of BCZY using RA route is $T=1100\text{ }^{\circ}\text{C}$.

Our previous work on the preparation of BCZY using various types of surfactants by route RB (Mazlan et al, 2015) showed that the samples of RB1, RB2, and RB3 have successfully formed a single-perovskite phase of cerate-zirconate compound after calcined at $T = 1100\text{ }^{\circ}\text{C}$. In this work, we further study on the reduction of calcination temperature for these samples to determine the minimum temperature needed for each sample to form single-perovskite BCZY phase. Figure 2 represent the close observation of XRD for prepared BCZY samples after calcined at $T= 950\text{ }^{\circ}\text{C}$. As shown, RB1 powder formed single-perovskite phase while other samples (RB2 and RB3) exhibited secondary impurities of BaCeO_3 , and BaZrO_3 oxides. These results might due to the insufficient energy to substitute Ce^{4+} ions into Zr^{4+} sites and vice versa leads to the formation of secondary phases. A reduction about 150 $^{\circ}\text{C}$ in the calcination temperature compared to RA1 showed that the RB1 produced single-phase of BCZY at lower processing temperature. From the XRD results, the average crystallite size, D , for samples RA1, RA2 and RB1 were estimated based on the Scherrer formula and summarized in Table 1. It was found that sample RB1 obtained smallest crystallite size indicated that Brij-97 as surfactant does not give any significant effect on crystallite size as well as lattice parameter of BCZY electrolyte rather assisting more uniform and homogenous particles (Changlin et. al. 2009). results, the average crystallite size, D , for samples RA1, RA2 and RB1 were estimated based on the Scherrer formula and summarized in Table 1. It was found that sample RB1 obtained smallest crystallite size indicated that Brij-97 as surfactant does not give any significant effect on crystallite size as well as lattice parameter of BCZY electrolyte rather assisting more uniform and homogenous particles (Changlin et. al. 2009).

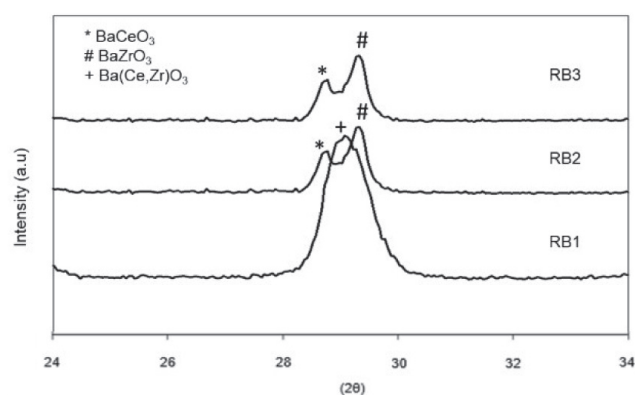


FIGURE 2. XRD spectra of the prepared BCZY sample with addition of various surfactant after calcined at $T= 950\text{ }^{\circ}\text{C}$.

TABLE 1. Crystallize size using Sherrer's equation.

Denomination of sample	Average crystallite size (nm)
RA1	79.50
RA2	77.75
RB1	74.62

The FESEM image of RA1 as in Figure 3 displayed spherical shape particles, dominated by agglomerates with the size in the range 342 – 396 nm. It is believed that during heat treatment (calcination process) of RA1 powder, the metal ions reacted with each other and fused together without any limitation and formed agglomerate BCZY particles.

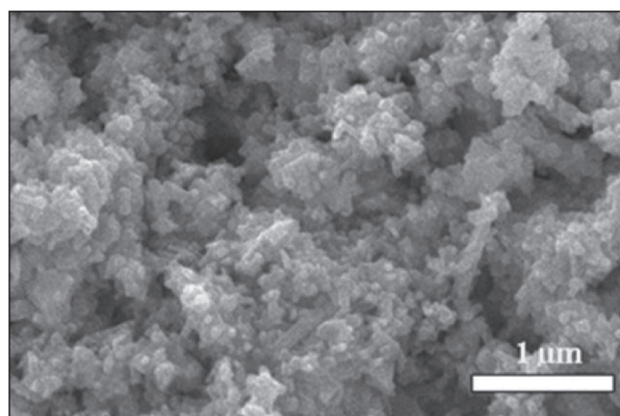


FIGURE 3. FESEM image of RA1 powder after calcined at T=1100 °C.

Figure 4 showed the FESEM images of all the samples prepared via RB route with spherical in shape. RB1 sample displayed spherical shape with particle size of 20 – 80 nm, while RB2 and RB3 dominated by agglomerates with size of 50 – 100 nm and 40 – 100 nm, respectively. The summary of particle size for each sample is listed in Table 2.

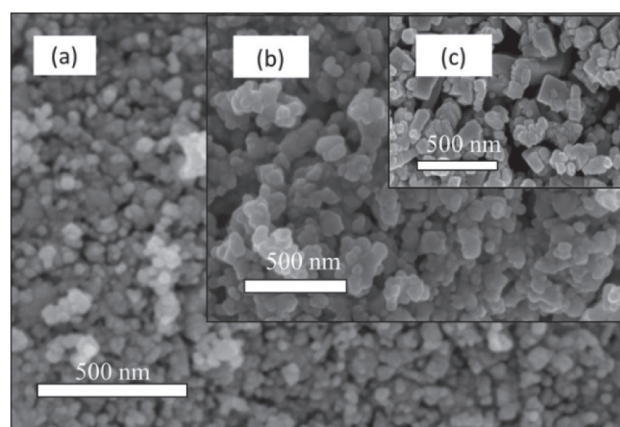
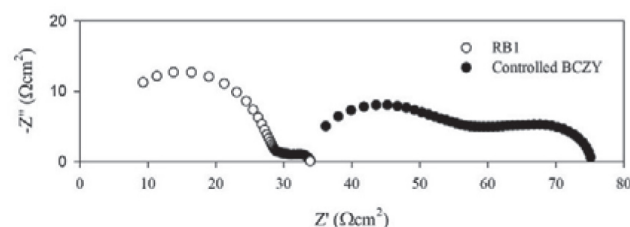


FIGURE 4. FESEM micrograph of BCZY sample with different surfactants after calcined at T= 950 °C; (a) RB1, (b) RB2, and (c) RB3.

TABLE 2. The particle size of BCZY powders prepared with different surfactants.

Denomination of sample	Particle size (nm)
RB1	20 – 80
RB2	50 – 100
RB3	40 – 100

The lower particle size of RB1 might be due to the surfactant's behavior or mechanism during the reaction process. The introduction of Brij-97 (non-ionic surfactant) during preparation of RB1 improves the dispersion property of the BCZY particles. This can be attributed to the favourable stability of the non-ionic surfactant micelles in aqueous solution, hence resulting a better interaction between the surfactant and BCZY particle, consequently prevent the aggregation of the sample (Huang et al. 2014).

FIGURE 5. Complex-impedance plane plots for (○) RB1 and (●) controlled BCZY pellet (prepared without surfactant) measured at T = 650 °C in wet N₂ atmosphere.

By means of low processing temperature and low agglomeration between all samples, sample RB1 is selected for further characterization. After sintered at T=1500 °C for 10 h, the relative density of RB1 pellet is ~90% and then subjected to impedance spectroscopy measurement in wet nitrogen atmosphere. At 650 °C the total conductivity of RB1 pellet is $2.40 \times 10^{-3} \text{ Scm}^{-1}$ compared to the controlled BCZY ($1.82 \times 10^{-3} \text{ Scm}^{-1}$) (Affandi et. al. 2018) as shown in Figure 5.

Following the impedance measurements, cross-sectional image of RB1 pellet is observed under FESEM as shown in Figure 6. Grains size analysis is done using ImageJ software and their size is ~90 nm in average. Grains of RB1 still retained in nano-ranged region, which likely the reason for lower conductivity value in comparison to the controlled BCZY. The obtained lower resistance is in agreement with several studies for sample with grain size < 100 nm (Li et al. 2011). The grain and grain boundary resistivity effects in nanocrystalline is smaller than that of microcrystalline materials, although the number of grain boundaries per unit length increases in smaller grain size condition and eventually provide smaller resistance value for nano-sized sample (Avila-Paredas et al. 2010).

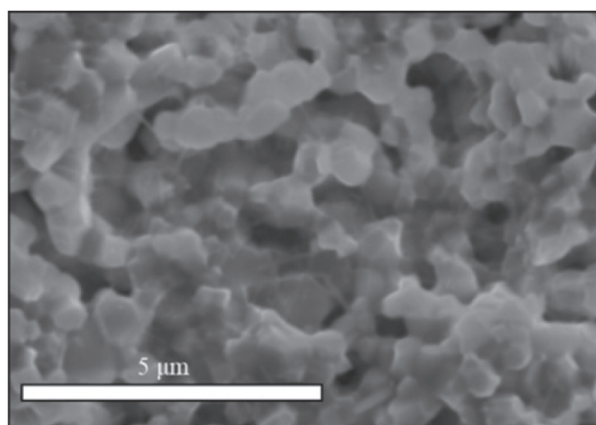


FIGURE 6. Cross-sectional SEM image of RB1 pellet after impedance measurements.

CONCLUSION

Single-phase of $\text{BaCe}_{0.54}\text{Zr}_{0.36}\text{Y}_{0.1}\text{O}_{3-\delta}$ (BCZY) powders are successfully prepared via a two different modified sol-gel routes. RB1 is selected for further characterization since it exhibited lower processing temperature and agglomeration of BCZY powder. As compared to a controlled BCZY, impedance measurements of sample RB1 exhibited higher conductivity value of $2.40 \times 10^{-3} \text{ Scm}^{-1}$ at $650 \text{ }^\circ\text{C}$ in wet nitrogen atmosphere. In conclusion, the employment of Brij-97 as the surfactant proved a new synthesis pathway for BCZY electrolyte which enable the reduced of processing temperature and particle size.

ACKNOWLEDGEMENT

This study is financially supported by the Ministry of Education (MoE) for the Grant Trans Disiplinary Research Grant 2016 (600-IRMI/TRGS 5/3 (001/2016)-2). Authors also thanks the University Teknologi MARA for facilities and supports

REFERENCES

- Abdullah, N. A., Osman, N., Hasan, S. & Hassan, O. H. 2012. Chelating agents role on thermal characteristics and phase formation of modified cerate-zirconate via sol-gel synthesis route. *International Journal of Electrochemical Science*, 7: 9401-9409.
- Abdullah, N. A. F. & Ang, L. S. 2018. Binding sites of deprotonated citric acid and ethylenediaminetetraacetic acid in the chelation with Ba^{2+} , Y^{3+} , and Ar^{4+} and their electronic properties: a density functional theory study. *Acta Chimica Slovenica* 65(1): 231-238.
- Affandi, N. S. M., Osman, N. & Hassan, O. H. 2018. A.C. conductivity of $\text{BaCe}_{0.54}\text{Zr}_{0.36}\text{Y}_{0.1}\text{O}_{3-\delta}$ electrolyte in dry and wet nitrogen atmospheres. *AIP Conference Proceedings* 2031(1): 020018.
- Avila-Paredes, H. J., Zhao, J., Wang, S., Pietrowski, M., Souza, R. A., Reinholdt, A. & Kim, S. 2010. Protonic

conductivity of nano-structured yttria-stabilized zirconia: Dependence on grain size. *Journal of Materials Chemistry* 20(5): 990-994.

- Baharuddin, N. A. & Andanastuti, M. 2018. Bilayered electrolyte for intermediate-low temperature solid oxide fuel cell: A review. *Jurnal Kejuruteraan SI* 1(2): 1-8.
- Baral, A. K., Sungmin C., Byung K. K. & Jong-Ho L. 2014. Processing and characterizations of a novel proton-conducting $\text{BaCe}_{0.35}\text{Zr}_{0.50}\text{Y}_{0.15}\text{O}_{3-\delta}$ electrolyte and its nickel-based anode composite for anode-supported IT-SOFC. *Materials for Renewable and Sustainable Energy* 3: 35.
- Biasotto, G., Simões, A., Foschini, C., Antônio, S., Zaghete, M. & Varela, J. 2011. A novel synthesis of perovskite bismuth ferrite nanoparticles. *Processing and Application of Ceramics* 5(3): 171-179.
- Fu, X., Luo, J., Sanger, A. R., Luo, N. & Chuang, K. T. 2010. Y-doped $\text{BaCeO}_{3-\delta}$ nanopowders as proton-conducting electrolyte materials for ethane fuel cells to co-generate ethylene and electricity. *Journal of Power Sources* 195(9): 2659-2663.
- Huang, G., Xu, S., Li, L. & Wang, X. 2014. Effect of surfactants on dispersion property and morphology of nano-sized nickel powders. *Transactions of Nonferrous Metals Society of China* 24(11): 3739-3746.
- Ke, S., Wang, Y. & Pan, Z. 2015. Effects of precipitant and surfactant on co-precipitation synthesis of $\text{Nd}_2\text{Si}_2\text{O}_7$ ceramic pigment. *Dyes and Pigments* 118: 145-151.
- Kreuer, K. D. 1997. On the development of proton conducting materials for technological applications. *Solid State Ionics* 97(1-4): 1-15.
- Kreuer, K. D. 1999. Aspects of the formation and mobility of protonic charge carriers and the stability of perovskite-type oxides. *Solid State Ionics* 125(1-4): 285-302.
- Kreuer, K. D. 2003. Proton-conducting oxides. *Annual Review of Materials Research*, 33(1): 333-59.
- Li, C., Gu, X., Wang, Y., Wang, Y., Liu, X. & Lu, G. 2009. Synthesis and characterization of mesostructured ceria-zirconia solid solution. *Journal of Rare Earths* 27(2): 211-215.
- Li, R., Zhen, Q., Drache, M., Rubbens, A., Estournes, C. & Vannier, R. 2011. Synthesis and ion conductivity of $(\text{Bi}_2\text{O}_3)_{0.75}(\text{Dy}_2\text{O}_3)_{0.25}$ ceramics with grain sizes from the nano to the micro scale. *Solid State Ionics* 198(1): 6-15.
- Liu, X., Zhang, Y., Yi, S., Huang, C., Liao, J., Li, H. & Tao, H. 2011. Preparation of V_2O_3 nanopowders by supercritical fluid reduction. *The Journal of Supercritical Fluids* 56(2): 194-200.
- Lyagaeva, J., Antonov, B., Dunyushkina, L., Kuimov, V., Medvedev, D., Demin, A. & Tsiakaras, P. 2016. Acceptor doping effects on microstructure, thermal and electrical properties of proton-conducting $\text{BaCe}_{0.5}\text{Zr}_{0.3}\text{Ln}_{0.2}\text{O}_{3-\delta}$ (Ln = Yb, Gd, Sm, Nd, La or Y) ceramics for solid oxide fuel cell applications. *Electrochimica Acta* 192: 80-88.
- Norman, N. W., Yusoff, W. N. A. W., Samat, A. A. & Andanastuti, M. 2018. Preparation of

- $\text{Sr}_{0.6}\text{Ba}_{0.4}\text{Ce}_{0.9}\text{Ga}_{0.1}\text{O}_{3-\delta}$ electrolyte pellets by glycine-nitrate method for proton-conducting solid oxide fuel cell applications. *Jurnal Kejuruteraan SI* 1(2): 33-39.
- Mazlan, N. A., Osman, N., Md Jani, A. M. & Yaakob, M. H. 2015. Role of ionic and nonionic surfactant on the phase formation and morphology of $\text{Ba}(\text{Ce,Zr})\text{O}_3$ solid solution. *Journal of Sol-Gel Science and Technology* 78(1): 50-59.
- Reverchon, E. & Adami, R. 2006. Nanomaterials and supercritical fluids. *The Journal of Supercritical Fluids* 37(1): 1-22.
- Ricote, S., Bonanos, N., Manerbino, A. & Coors, W. 2012. Conductivity study of dense $\text{BaCe}_x\text{Zr}_{(0.9-x)}\text{Y}_{0.1}\text{O}_{(3-\delta)}$ prepared by solid state reactive sintering at 1500 °C. *International Journal of Hydrogen Energy* 37(9): 7954-7961.
- Senari, S. M., Osman, N. & Md Jani, A. M. 2017. Characterization of NiO-BCZY composite anode prepared by one-step sol-gel method. *International Conference on Solid State Science and Technology 2017 Proceeding* 25(1): 135-141.